# New stratospheric dust belt due to the Chelyabinsk bolide

Nick Gorkavyi,[1] D. F. Rault,[2] P. A. Newman,[3] A. M. da Silva,[3] and A. E. Dudorov[4]

Received 11 June 2013; revised 17 July 2013; accepted 24 July 2013; published 5 September 2013.

[1] The Ozone Mapping Profiler Suite (OMPS) Limb Profiler (LP) on the recently launched NASA/NOAA NPP/Suomi satellite detected aerosol excess in the mid-stratosphere (25–45 km altitude) between 50°N and 70°N latitudes. OMPS/LP observations trace this aerosol plume to the meteor that struck near Chelyabinsk, Russia on 15 February 2013. This new dust layer, located above the Junge aerosol layer, has persisted over at least a 3 month period. Material collected on the ground following the bolide explosion showed that the meteor was mostly composed of olivine and pyroxenes. Simulations using Lagrangian and Eulerian atmospheric models trace the plume back to Chelyabinsk and confirm that the plume altitude was at altitudes between 25 and 45 km. The models also confirm the plume circumpolar longitudinal spreading observed by OMPS/LP, with propagation speeds up to 85 m/s.
**Citation:** Gorkavyi, N., D. F. Rault, P. A. Newman, A. M. da Silva, and A. E. Dudorov (2013), New stratospheric dust belt due to the Chelyabinsk bolide, *Geophys. Res. Lett.*, *40*, 4728–4733, doi:10.1002/grl.50788.

## 1. Introduction

[2] The primary goal of the OMPS/LP sensor is to assess the 3-D distributions of ozone and stratospheric aerosol in the Earth's mid-atmosphere. The OMPS/LP measures limb-scattered light at high vertical resolution 1.5–2 km, high sampling rate at one measurement per degree latitude, 7000 measurements per day, and on a 5 day repetition rate [*Flynn et al*., 2007; *Rault and Loughman*, 2013]. The NPP/Suomi satellite operates in a near-circular, sun-synchronous orbit with a 1:30 P.M. ascending node—making the aerosol retrieval particularly sensitive at high northern latitudes. OMPS/LP retrieved the aerosol extinction with an estimated 30% precision, using wavelengths ranging from 470 to 870 nm. The aerosol extinction parameter is defined as the fractional reduction of sunlight for 1 km path. Information on aerosol particle size distribution is inferred from the spectral dependence of the extinction (Angstrom coefficient).

[3] The Chelyabinsk meteor about 18 m in diameter and weighing about 11,000 t entered the atmosphere at a velocity of 18.6 km/s. It exploded near Chelyabinsk on 15 February 2013 at 03:20 UT, at an altitude of 23.3 km with an energy release equivalent to more than 30 Hiroshima atomic weapons [*Yeomans and Chodas*, 2013]. The point of maximum brightness was located at 54.8°N and 61.1°E [*Yeomans and Chodas*, 2013]. According to the observations, most meteoritic dust was loaded on altitudes from 23 to 45 km. A significant fraction of the explosion debris was transported upwards in an air burst mushroom cloud which rose quickly in about 100 s up to 33–35 km, above the Earth's natural Junge aerosol layer [*Gorkavyi et al*., 2013]. On the ground, meteoritic debris scattered over a large area, and recovered fragments were found to be very small [*Badyukov and Dudorov*, 2013; *Dudorov et al*., 2013].

## 2. Observations

[4] The OMPS/LP instrument first observed the meteor plume on 15 February 2013 at altitudes above 40 km near Novosibirsk at 55°N, 80.7°E—about 1100 km east of Chelyabinsk region and 3 h 30 min after the meteor impact. This observation would imply an eastward plume drift velocity of ~85 m/s. On the next orbit, the NPP passed over Chelyabinsk at 8:26 UT (5 h 06 min after the event, 54°N–55°N, 63.8°E) and detected a dense cloud at ~30 km (see Figure S1 in the supporting information). On the next day, 16 February, OMPS/LP made its third observation of the plume at 3:10–6:30 UT, 1700–4300 km east of Chelyabinsk at longitudes from 88°E–141°E (see Figure S2). These observations are consistent with a mean eastward velocity ranges from 20 to 45 m/s. On 16 February, the plume was detected several times on succeeding orbits and was observed to stretch over 150° of longitude, reaching the Aleutian Island (Figure 1). The vertical wind shear as depicted by meteorological analysis at these levels is consistent with the observed plume stretching, with higher-altitude dust near 40 km moving much faster eastward than the lower altitude dust near 30 km (see Figure S3). On 18 February, the plume was observed from North America West Coast to the middle of the Atlantic Ocean with the maximum plume density registered along the US/Canada border at altitudes of 36–37 km. On 19 February, 4 days after meteor impact, the upper part of the meteor plume had circumnavigated the globe and returned over Chelyabinsk. In the following days, OMPS/LP frequently detected two layers at different altitudes, indicating that the upper altitude head had caught up with the lower altitude tail of the plume. By the end of February, the meteoric dust plume had formed a quasicontinuous midlatitude belt located a few kilometers above the Junge layer. While the extinction in this belt is about 10 times smaller than the lower altitude Junge layer value, it can nevertheless be detected by limb viewing sensors such as OMPS/LP sensor. Figure 2 depicts a series of extinction vertical profiles for the meteor plume and the

Additional supporting information may be found in the online version of this article.

[1]Science Systems and Applications, Inc., Lanham, Maryland, USA.
[2]Morgan State University, Columbia, Maryland, USA.
[3]NASA Goddard Space Flight Center, Greenbelt, Maryland, USA.
[4]Chelyabinsk State University, Chelyabinsk, Russia.

Corresponding author: N. Gorkavyi, Science Systems and Applications, Inc., Suite 600, 10210 Greenbelt Rd., Lanham, MD 20760, USA. (nick.gorkavyi@nasa.gov)


0094-8276/13/10.1002/grl.50788

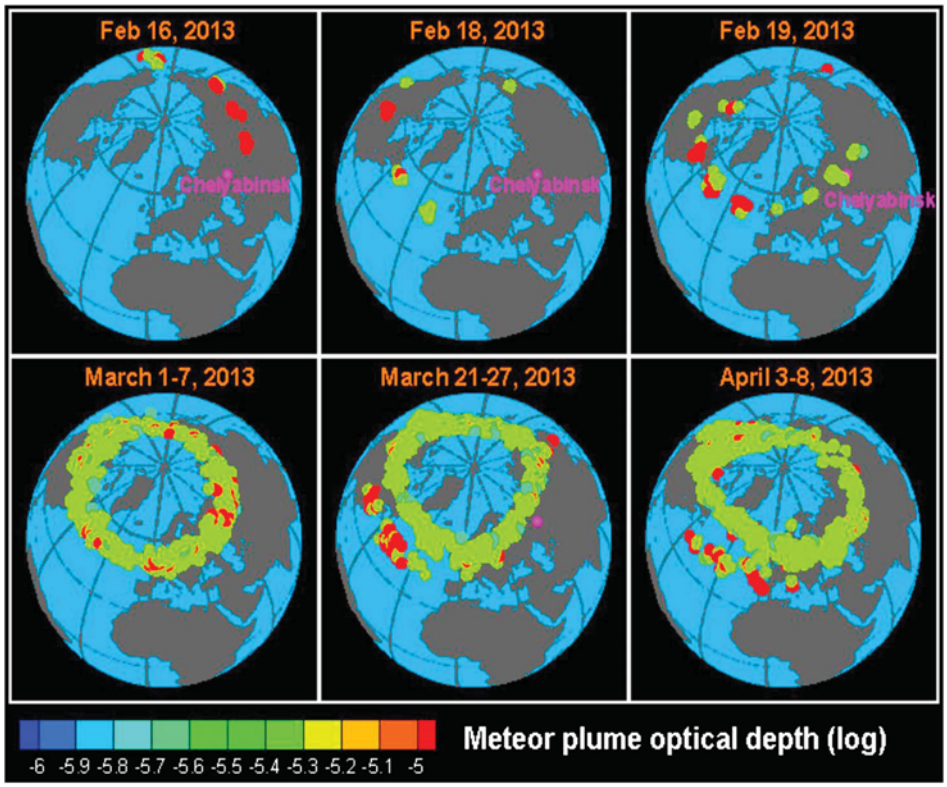


**Figure 1.** Meteor plume eastward progression and formation of the belt. Each OMPS/LP observation corresponds to an orbital overpass, which typically occurs about every 25° longitude. The shape of the belt is tied to the polar vortex as confirmed by the GEOS-5 model simulations. A new dust structure can be seen to form in late March over the North Atlantic region. This second structure is "aerosol bubble" which was splitted from tropical Junge layer.

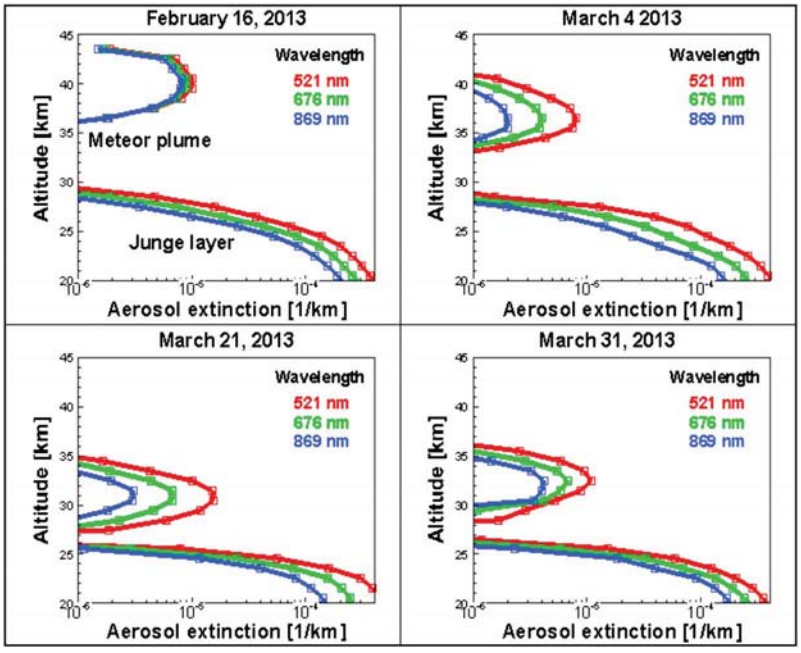


**Figure 2.** Extinction profiles within the Chelyabinsk meteor dust plume. The extinction spectral dependence is an indicator of particle size: little spectral dependence indicates the presence of large particles (such as on 16 February), whereas larger spectral dependence points to smaller particles (as in later days). The sensitivity of the OMPS/LP instrument can be estimated as $3 \times 10^{-6}$ 1/km.

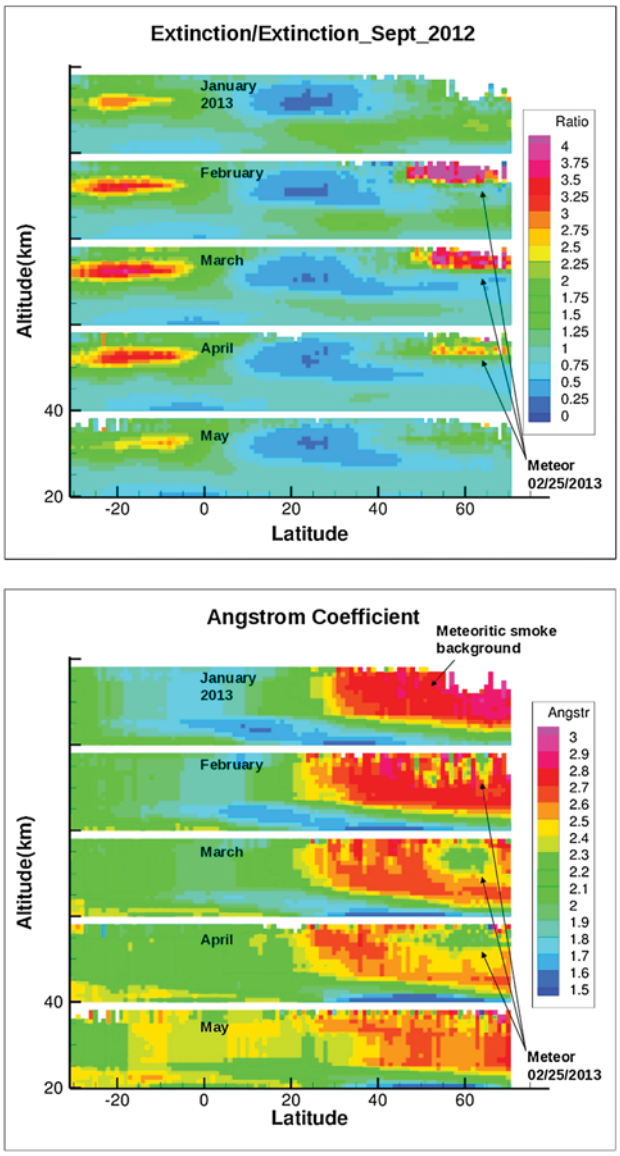


**Figure 3.** Time evolution of the meteor dust layer. (top) Ratio of zonal mean of extinction coefficient for different months to background month September 2012. (bottom) Angstrom coefficient for different months. Population of small particles at altitudes > 30 km and latitudes > 30°N–40°N is a background from meteoritic dust (see the plot for January). Meteor belt is different from seasonal variations of extinction and Angstrom coefficient.

Junge layer for a series of days. Figure 3 shows the time evolution of the meteor belt as viewed by the OMPS/LP sensor over the 3 months after meteor impact. Figure S4 shows that the meteor dust layer is slowly descending towards the Junge layer at a rate of about 90 m/day under the effect of sedimentation and diabatic cooling [*Gerding et al.*, 2003], with particles slowly decreasing in size, from 0.2 micron (Angstrom coefficient = 0) down to 0.05 micron (Angstrom coefficient = 3). Its optical depth also very slowly decreased. The belt has a vertical depth of about 5 km, a width of about 300–400 km.

[5] The chemical composition and optical properties of the meteoric dust can be inferred from the rather large ensemble of samples that were collected on the ground both in the form of small meteorites and meteoritic dust (Figures 4 and S5). The recovered meteoritic material consists of ordinary chondrite LL5 with the following chemical composition [*Dudorov et al.*, 2013]: (a) Olivine $(Mg, Fe)_2SiO_4$ = 45,5%, (b) pyroxenes $Ca(Mg, Fe, Ai)(Si,Al)_2O_6$ = 34%, and (c) ferric oxide $Fe_2O_3$ = 17.5%.

## 3. Modeling and Simulations

[6] The stratospheric dust transport is simulated using Lagrangian trajectory models and a global Eulerian transport model. The Goddard Trajectory Model [*Schoeberl and Sparling*, 1995] has been employed to track volcanic plumes in both the stratosphere and upper troposphere [*Krotkov et al.*, 2010; *Schoeberl et al.*, 1993] and to track a stratospheric rocket launch plume that drifted from the Baikonur Cosmodrome to California [*Newman et al.*, 2001]. The trajectories are driven using the wind and temperatures from NASA's Modern Era Retrospective Analysis for Research and Applications reanalysis [*Rienecker et al.*, 2011]. Parcels are initialized in a cylinder extending from 33.5 to 43.5 km (which OMPS/LP has identified as the plume's densest part) in a circle with a 150 km radius centered on Chelyabinsk at 03:20 UT on 15 February. In the simulation, parcels move rapidly in an east-northeast direction from Chelyabinsk following the explosion. Figure 5 displays the initial location of the parcels (the white circle), and the trajectory distributions on 16 February at 3:00 UT, 16 February at 23:00 UT, 18 February at 16:00 UT, and 20 February at 12:00 UT. On 16 February, the cylinder has developed into an elongated structure that tilts eastward with altitude, with the parcels extending considerably eastward of Chelyabinsk. The high-extinction OMPS/LP observations are nearly coincident with the trajectories. The higher-altitude trajectories reached Alaska very late on 16 February and were over Canada on 17 February. On 20 February, the trajectories extended in a long arc from Canada, across the North Atlantic into Europe, and across the Russian Federation. Superimposed on Figure 5 are the OMPS/LP observations that showed large extinction ($> 1.0 \times 10^{-6}$ 1/km) that were above 31 km (peak extinction altitude is colored on the same color scale as the trajectories). The trajectories match these extinction locations quite well (errors of less than 300 km horizontally and 3 km vertically) over the 5 day period shown on Figure 5.

[7] The Goddard Earth Observing System Version 5 (GEOS-5) is the latest version of the NASA Global Modeling and Assimilation Office Earth system model [*Rienecker et al.*, 2008]. GEOS-5 contains components for atmospheric circulation and composition (including atmospheric data assimilation), with aerosol processes derived from the Goddard Chemistry Aerosol Radiation and Transport model [*Chin et al.*, 2002; *Colarco et al.*, 2010]. The near real-time version of GEOS-5 used for the bolide dust simulations runs on a global 25 km cubed sphere grid [*Putman and Suarez*, 2011] with 72 vertical levels having the model top at 0.01 hPa (~80 km) and is informed by the full tropospheric and stratospheric meteorological data assimilation. We have customized the dust component of GEOS-5 for simulating the meteoric dust plume by adjusting the size range of the five dust bins to accommodate submicron particles with central radius at 0.06, 0.11,

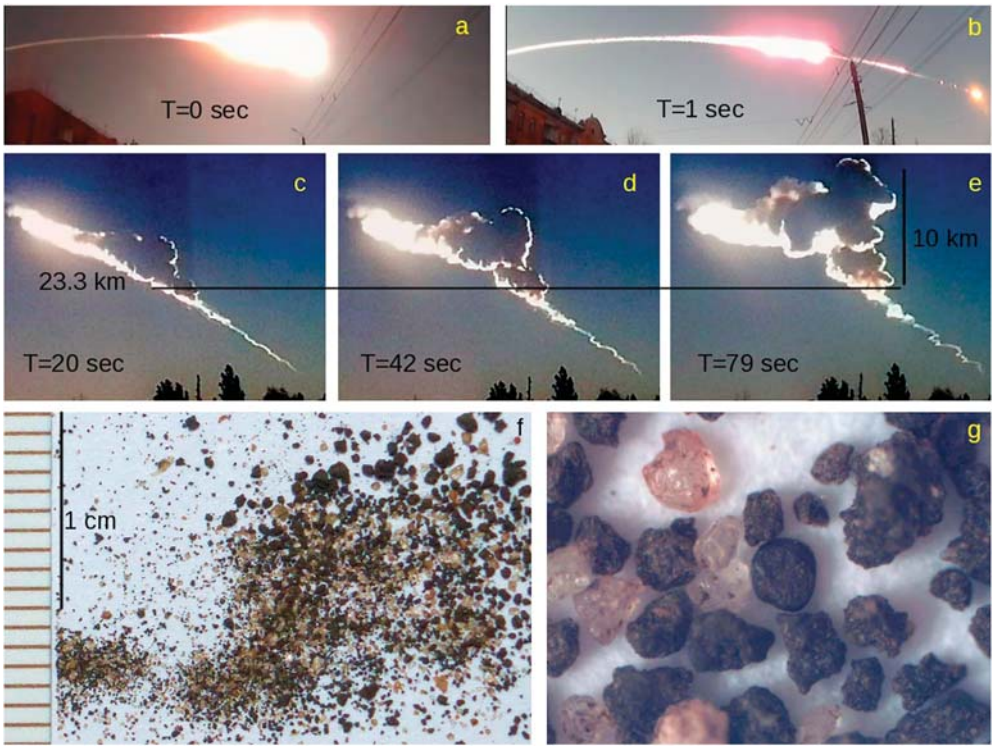


**Figure 4.** (a, b) View of the meteor from Chelyabinsk (video by Sergei Zhabin). (c–e) Evolution of the plume after the blast (photos by Sergei Vladelschikov, Kusa). (f, g) Fine meteoritic dust which were collected on snow after the blast. Figure 4g shows the photo by microscope.

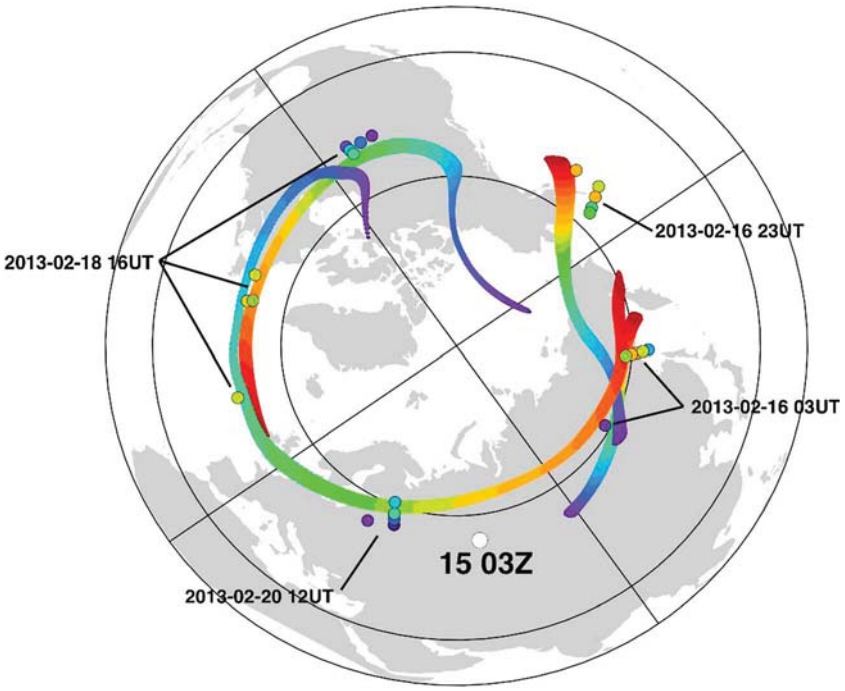


**Figure 5.** Trajectories (purple coloring) originated from a cylinder of parcels that were initialized on 15 February at the location of the Chelyabinsk bolide (white circle). Trajectories at the lower altitude (darker purple, 33.5 km) are on the western edges of the parcel collections, while the trajectories at the higher altitude (red, 43.5 km) are on the eastern edges. The OMPS/LP profiles with extinctions greater than $1.0 \times 10^{-6}$ are indicated by the colored circles (higher altitudes in red and lower altitudes in purple as with the trajectories).

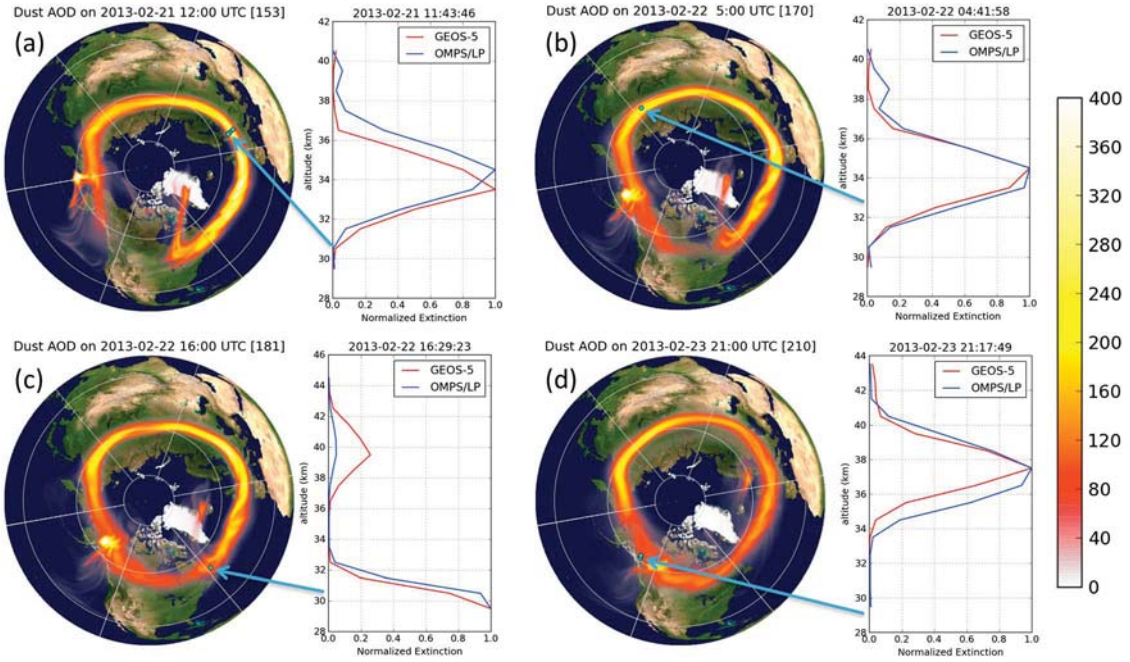


**Figure 6.** GEOS-5 simulated meteoric dust optical depth (AOD) about 1 week after initialization on (a) 11:30 UT 21 February 2013, (b) 16:30 UT 22 February 2013, (c) 4:30 UT 22 February 2013, and (d) 21:30 UT 23 February 2013. The blue dots represent the location of the OMPS/LP retrieval where the modeled and observed vertical structure of the plume is compared. The normalized extinction is defined by scaling the extinction profiles by its maximum value above 30 km. The color bar is for aerosol AOD scaled by $10^6$.

0.22, 0.44, and 0.89 μm. The five dust tracers run coupled to the GEOS-5 radiation parameterization and are subject to the standard GEOS-5 dust processes: advection, diffusion, convective transport, dry/wet deposition, and sedimentation. The initial dust mass distribution on 3:20 UT 15 February 2013 are prescribed based on a parametric model centered on Chelyabinsk with initial mass distribution of 100 t between 15–60 km, with most of the mass between 30 and 40km, peaking around 35 km. This total mass was distributed among the five bins, with 80% of the mass equally assigned the three smallest bins and 20% to two largest bins. For these initial simulations, we have retained the standard dust optical properties in GEOS-5, which are based on Optical Properties of Aerosols and Clouds database [*Hess et al*., 1998] and roughly agree with the index of refraction reported for the Bruderheim meteorite [*Egan and Hilgeman*, 1979]. A movie is included in the supporting information depicting the time evolution of the modeled dust plume. A distinct dust plume emanating from Chelyabinsk is oriented in the zonal direction until it reaches North America around 23:00 UT on 16 February when its leading edge acquires a north–south orientation associated with a stratospheric ridge located to west of the Aleutian islands. As the plume exits North America, it again acquires a zonal orientation reaching its circumpolar nature around 22 February. Snapshots of the modeled plume about a week after initialization are shown in Figure 6 superimposed with the location of OMPS/LP retrievals. The model captures well the horizontal location of the observed plume as well as its vertical structure. By 25 February, a fully developed belt is established with portions of the plume having a bimodal structure (not shown).

## 4. Conclusions

[8] The Chelyabinsk meteor event ranks among the largest bolide events ever recorded (the following are examples of largest bolides from last century: Tungiska, 1908; Brazilian bolide, 1930; Bolide in Spain, 1932; South African bolide, 1963). For that event, the OMPS/LP instrument has proven to be a valuable tool allowing the science community to track the meteor plume in time and space and document its effects on the atmosphere. Furthermore, the current state of models and stratospheric meteorological data assimilation permit skillful prediction of the evolution meteoric dust plumes suggesting a great potential for the assimilation OMPS/LP aerosol retrievals in near real time.

[9] The Earth is constantly impacted by meteors, and meteoric debris are known to contribute to high-altitude atmospheric physics (such as condensation nuclei for stratospheric and mesospheric clouds). These effects are still not well characterized, and it is hoped that further observations by OMPS/LP over its 5 year design lifetime will help in better understanding these effects. OMPS/LP could be used to scrutinize the upper atmosphere above the Junge layer in search for meteor debris, which will then allow one to (1) identify hitherto unobservable meteor events and (2) provide the needed information on meteoric dust to the atmospheric science community.

[10] **Acknowledgments.** We particularly wish to thank J. Gleason and P. Bhartia for their support. We also recognize contributions from the OMPS/LP processing team, especially J. Warner and T. Zhu. Special thanks also are due to a team of scientists at Chelyabinsk State University, especially A. Yu. Shatin, A. V. Melnikov, S. V. Taskaev, V. A. Tyumentsev, S. N. Zamozdra, O. V. Eretnova, S. A. Khaibrakhmanov, and A. V. Kocherov.

P. Colarco provided the dust optical properties used in the GEOS-5 simulations.

[11] The Editor thanks two anonymous reviewers for their assistance in evaluating this paper.

## References

Badyukov, D. D., and A. E. Dudorov (2013), International Geochemistry, 51.

Chin, M., et al. (2002), Tropospheric aerosol optical thickness from the GOCART model and comparisons with satellite and sunphotometer measurements, *J. Atmos. Sci.*, *59*, 461.

Colarco, P., A. da Silva, M. Chin and T. Diehl (2010), Online simulations of global aerosol distributions in the NASA GEOS-4 model and comparisons to satellite and ground-based aerosol optical depth, *J. Geophys. Res.*, *115*, D14207, doi:10.1029/2009JD012820.

Dudorov, A. E., et al. (2013), Proc. of the Chelyabinsk State University, Physics, 17.

Egan, W. G., and T. W. Hilgeman (1979), *Optical Properties of Inhomogeneous Materials*, Academy Press, New York.

Flynn, L. E., C. J. Seftor, J. C. Larsen, and P. Xu (2007), The Ozone Mapping and Profiler Suite (OMPS), Earth Science Satellite Remote Sensing, Springer-Verlag and Tsinghua University Press.

Gerding, M., et al. (2003), Observation of an unusual mid-stratospheric aerosol layer in the Arctic: Possible sources and implications for polar vortex dynamics, *Annales Geophys.*, *21*, 1057.

Gorkavyi, N., T. A. Taidakova, E. A. Provornikova, I. Gorkavyi, and M. M. Akhmetvaleev (2013), Aerosol plume after the Chelyabinsk bolide, *Sol. Syst. Res.*, *47*(N4), 275.

Hess, M., P. Koepke, and I. Schult (1998), Optical Properties of Aerosols and Clouds: The software package OPAC, *Bull. Am. Meteorol. Soc.*, *79*, 831, doi:10.1175/1520-0477(1998)079<0831:OPOAAC>2.0.CO;2.

Krotkov, N. A., M. R. Schoeberl, G. A. Morris, S. Carn, and K. Yang (2010), Dispersion and lifetime of the $SO_2$ cloud from the August 2008 Kasatochi eruption, *J. Geophys. Res.*, *115*, D00L20, doi:10.1029/2010JD013984.

Newman, P. A., J. C. Wilson, M. N. Rossa, C. A. Brock, P. J. Sheridan, M. R. Schoeber1, L. R. Lair, T. P. Bui, M. Loewenstein, and J. R. Podolske (2001), Chance encounter with a stratospheric kerosene rocket plume from Russia over California, *Geophys. Res. Lett.*, *28*, 959–962, doi:10.1029/2000GL011972.

Putman, W. M., and M. Suarez (2011), Cloud-system resolving simulations with the NASA Goddard Earth Observing System global atmospheric model (GEOS-5), *Geophys. Res. Lett.*, *38*, L16809, doi:10.1029/2011GL048438.

Rault, D. F., and R. P. Loughman (2013), The OMPS Limb Profiler environmental data record algorithm theoretical basis document and expected performance, *IEEE Trans Geosci Rem Sens*, *51*(5), 2505–2527, doi:10.1109/TGRS.2012.2213093.

Rienecker, M. M., et al. (2008), The GEOS-5 Data Assimilation System—Documentation of Version 5.0.1, 5.1.0, and 5.2.0., NASA Technical Report Series on Global Modeling and Data Assimilation, 27.

Rienecker, M. M., et al. (2011), MERRA—NASA's Modern Era Retrospective Analysis for Research and Applications, *J. Clim.*, *24*, 3624, doi:10.1175/JCLI-D-11-00015.1.

Schoeberl, M. R., and L. Sparling (1995), In diagnostic tools in atmospheric physics, Proc. Int. School Phys. "Enrico Fermi", vol. 124, edited by G. Fiocco and G. Visconti, 289 pp., Soc. Ital. di Fis., Bologna, Italy.

Schoeberl, M. R., S. Doiron, L. R. Lait, P. A. Newman, and A. J. Krueger (1993), A simulation of the Cerro Hudson $SO_2$ cloud, *J. Geophys. Res.*, *98*, 2949–2955, doi:10.1029/92JD02517.

Yeomans, D., and P. Chodas (2013), Additional details on the large fireball event over Russia on Feb. 15, 2013. NASA/JPL, March 1 http://neo.jpl.nasa.gov/news/fireball_130301.html.